



## MULTISCROLL ATTRACTORS IN SEMICONDUCTOR LASER BY OPTICAL FEEDBACK AND DIRECT CURRENT MODULATION

<sup>1</sup>Nasraldien. A. Eashag Saeed, <sup>2</sup>Awadelgied A. M., <sup>3</sup>Abdalah S.F., <sup>4</sup>Al Naimee K.A.,

<sup>1</sup>Physics Dept, College of Education, Nyala University, Nyala, Sudan

<sup>2</sup>Karaya University, Khartoum Sudan

<sup>3</sup>CNR-Istituto Nazionale di Ottica, Largo E. Fermi 6,50125, Firenze, Italy

<sup>4</sup>CNR-Istituto Nazionale di Ottica, Largo E. Fermi 6,50125, Firenze, Italy, Department of physics, College of Science, University of Baghdad, Baghdad, Iraq

### ABSTRACT

Chaotic behavior with multiscroll attractors and equilibrium points of semiconductor laser dynamics subjected to optical delay feedback and sinusoidal injection current modulation observed numerically. The complicated dynamical behavior performed based on numerical simulation of modified Lang-Kobayashi model with direct current modulation term. The results reveal different dynamical regimes involving steady state, periodic, quas-periodic, mixed modes, chaotic state with high power and 1-D 10 scroll attractors. These dynamics analyzed by sequences of observation analysis, FFT, phase portrait in two and three dimensions that qualify sensitivity of the system to initial conditions and give measure of the rate at which the trajectories separate one from the other (fixed point attractor). These prove important use in Chaos synchronization and networks

**KEYWORDS:** Semiconductor Laser Nonlinear Dynamics; Time Delay Optical Feedback; Modulation

### INTRODUCTION

Chaos generation and control in nonlinear differential equations and devices to reach such dynamical behavior have been proposed. Among these is semiconductor laser. From the point of view of nonlinear dynamics and chaos generation are very sensitive to external perturbations as a nonlinear interaction of the light with laser medium which can be utilized to stabilize or destabilize semiconductor laser dynamics. These dynamics of semiconductor lasers are formulated by nonlinear system differential equations. Depending on the types of optical feedback, optical feedback strength, external cavity length and injection current [1], many nonlinear dynamical phenomena are occurred, such as multistability [2], instability, self pulsation [3] and coherence collapse. The output power displays, steady state, regular and irregular oscillations separated by different time intervals with sudden dropouts high chaotic spiking, strange chaotic attractor [4]. Recently, different shapes of chaotic attractors have been generated in different successful methods reported in [5]-[8], one type is multiscroll chaotic attractors which are very much high complex dynamical behavior and classified into 1-D, 2-D, and 3-D scroll attractors, depending on the location of the equilibrium points in the

state space [9]. These perturbations have been received considerable theoretical and practical attraction involving optical delay feedback from distant mirror or optical fiber loop mirror [10], phase-conjugate feedback [11], optoelectron feedback [12], optoelectron feedback and modulation [13][14], optical injection [15]. These complex behaviors of chaotic attractors are used in great applications such as secure optical communication where confidential information embedded [16], chaotic lidars, random number generation and neural science [17]. In the following we investigate the effect of optical feedback strength in semiconductor laser dynamics. The model of coupled time delay differential equations for the rate of change of electric field amplitude, the carrier density and the optical phase. The model is referred to Lang and Kobayashi [18]. Depending on the modulation parameters and the internal laser parameters, the lasers exhibit complex chaotic behavior [19-20].

### DYNAMICAL MODEL AND METHOD

In the case of a two-dimensional dynamical system where chaotic dynamics cannot and for small-moderate and strong optical feedback strength; the dynamical model in [15] can be expressed in polar coordinates as:

$$\frac{dE}{dt} = \frac{1}{2} \left[ G(t) - \frac{1}{\gamma_p} \right] E + (k + \sigma) E(t - \tau) \cos(\omega\tau + \varphi(t) - \varphi(t - \tau)) + \sqrt{2\beta N(t)} X \dots (1.1)$$

$$\frac{d\varphi}{dt} = \frac{1}{2} \alpha \left[ G(t) - \frac{1}{\gamma_p} \right] - \frac{(k + \sigma) E(t - \tau)}{E} \sin(\omega\tau + \varphi(t) - \varphi(t - \tau)) \dots (1.2)$$

$$\frac{dN}{dt} = \frac{I}{e} - \gamma_c N - G(t)|E(t)|^2 \dots \dots \dots (1.3)$$

Where E stand for electric field amplitude, N is the carrier density,  $\varphi$  is optical phase, optical gain  $G(t) = \frac{g(N-N_{th})}{1+s|E(t)|^2}$ . In numerical simulation matlab we consider the initial conditions and parameters values as E ,N and  $\varphi = .001$ ,  $0.1$   $0.001$ , photon decay time  $\gamma_p = 1.93e-12$ , carrier decay time  $\gamma_c = 2e-9$  ,g is the gain coefficient  $g = 1.5e4$ , gain saturation coefficient  $s = 5e-7$ , current density injection  $J = 1.5$ , electric charge  $e = 1.6e-19$ , volume of active layer  $d =$  , carrier density at transparency  $N_{th} = 1.5e8$  , the linewidth enhancement factor  $\alpha = 3$ ,delay time  $\tau = 10e-9$  , Feedback strength  $k = 3.6e11$ , Injection strength  $\sigma = 40$ , Optical angular frequency\* delay time  $\omega\tau = 4.9077e6$  , spontaneous emission rate  $\beta = 1.6e3$  , Gaussian noise sources  $X= 1$ ,

$I=(i_{ac} + i_{ac} * \sin(2\pi f_m t))$  is modulation term,  $i_{dc}$  is direct current =10mA , $i_{ac}$  is amplitude or indirect current = 5mA,  $f_m$  is modulation frequency=  $100e^6$  Hz.

**RESULTS AND DISCUSSION**

The dynamical characteristics depending on the different values of optical feedback strength (km), where temporal evolution waveforms of semiconductor laser are analyses by time series with corresponding power spectrum FFT and phase space portrait with attractors are shown in fig(1-13).

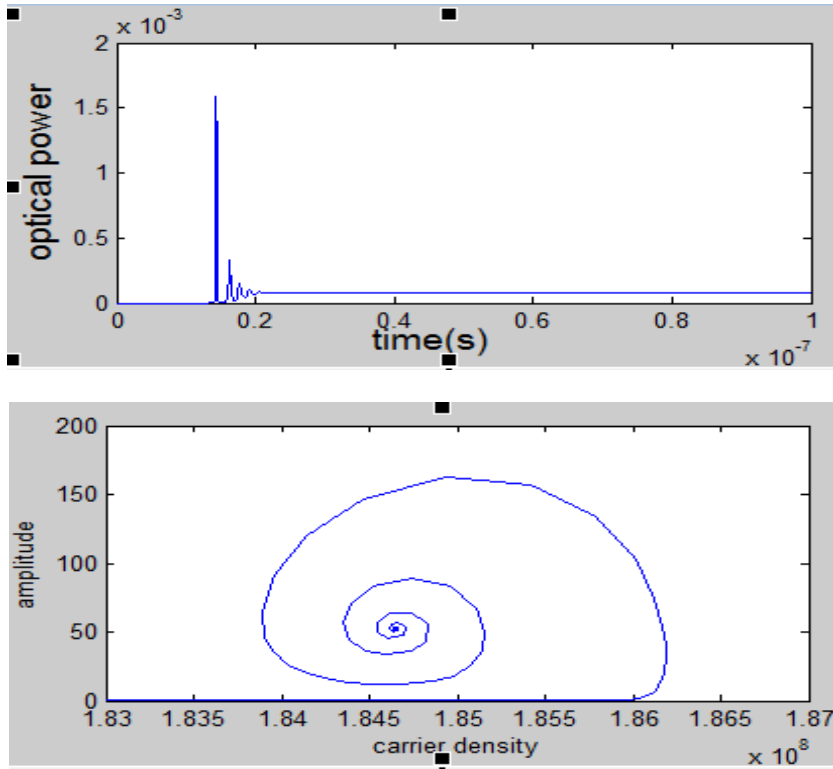
Fig.1&2 optical output operates high power and oscillated to steady state at very weak optical feedback strength ( $36e^{-10}ns^{-1}$  to  $36e^{-8}ns^{-1}$ ), it's corresponding FFT spectrum dynamic shows one high peak and number of equal peaks at different frequencies and it's attractor has orbits converge to fixed point(attracting fixed point).At optical feedback strength  $36e^{-6}ns^{-1}$  to  $36e^{-4} ns^{-1}$  fig.(3&4) show

same behavior. Fig. 5 characterized clear oscillations with one high peak, attractor point become denser than that when optical feedback strength increased near critical values. On the other hand, fig 6& 7 when the optical feedback strength equal ( $36e^{-1} ns^{-1}$ ) the temporal waveforms show complex behaviors rise out as number of irregular peaks in different time intervals where wide range frequencies and one large diameter orbit with some small diameter orbits generated in phase portrait plot [16], these large and small spikes separated by irregular time interval are associated with mixed mode [17] and at fig. (8 &9) ( $km = 36 ns^{-1}$ to  $360 ns^{-1}$ ) time series shows clear and very high chaotic spikes at ten breakpoints, and 1D 4 scroll attractors associated with number of homoclinic orbits to saddle focus point in the third and fourth scroll attractors appeared in phase space trajectory. The corresponding four transform illustrate high peaks in different frequencies.

Fig. 10 shows clear 1D 10 scroll attractors corresponding to that 10 breakpoints appeared in time series when plot the same results in fig. 9 in three dimensions. By using for loop of optical feedback strength and iterated solutions in matlab we obtained very high density 1D 10 scroll attractors and time series as fig.(11 &12).

Fig. 13 shows 1-D 10 scroll attractors in three dimensions phase space portrait for three different values of initial conditions.

The whole evolutions of semiconductor laser dynamics from periodic at low optical feedback strength periodicity, number of spikes, amplitude power, to high chaotic state where multi-scroll attractors appears are increasing by increasing optical feedback strength.



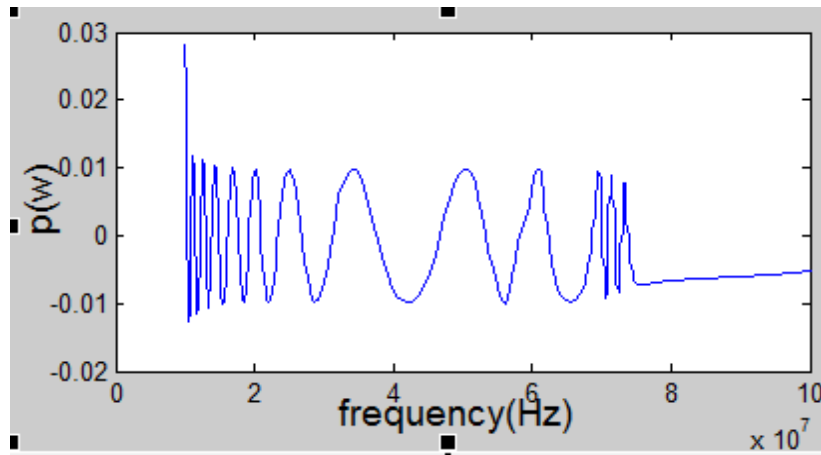


Fig. 1 time series of the laser output power, its phase portrait and corresponding FFT spectrum. at  $k = 36e^{-10}ns^{-1}$ ,  $i_{dc} = 10mA$ ,  $i_{ac} = 5mA$ ,  $f_m = 100e^6$  Hz.

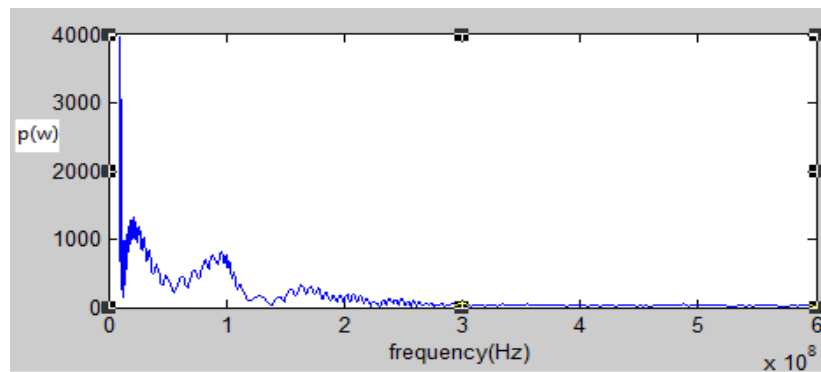
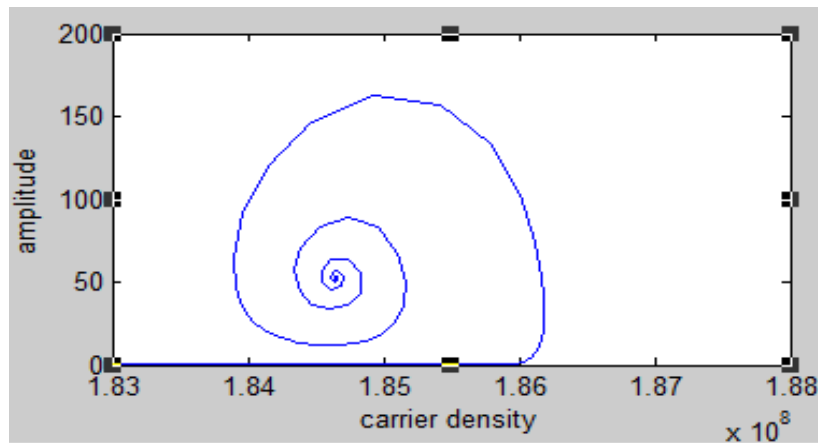
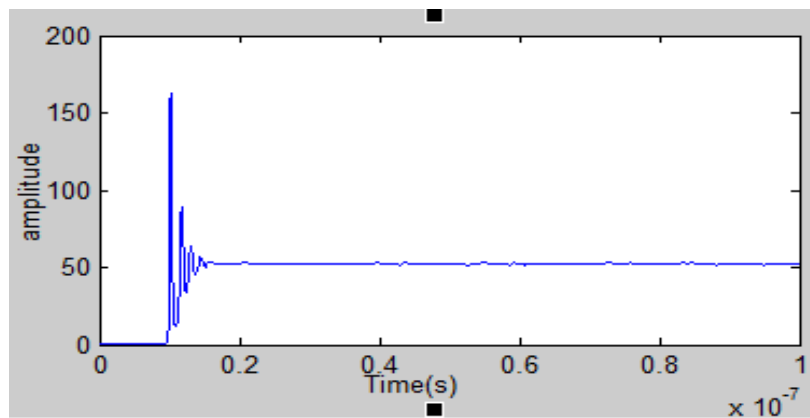


Fig. 2 time series of the laser output power, its phase portrait and corresponding FFT spectrum. at  $k = 36e^{-8}ns^{-1}$ ,  $i_{dc} = 10mA$ ,  $i_{ac} = 5mA$ ,  $f_m = 100e^6$  Hz.

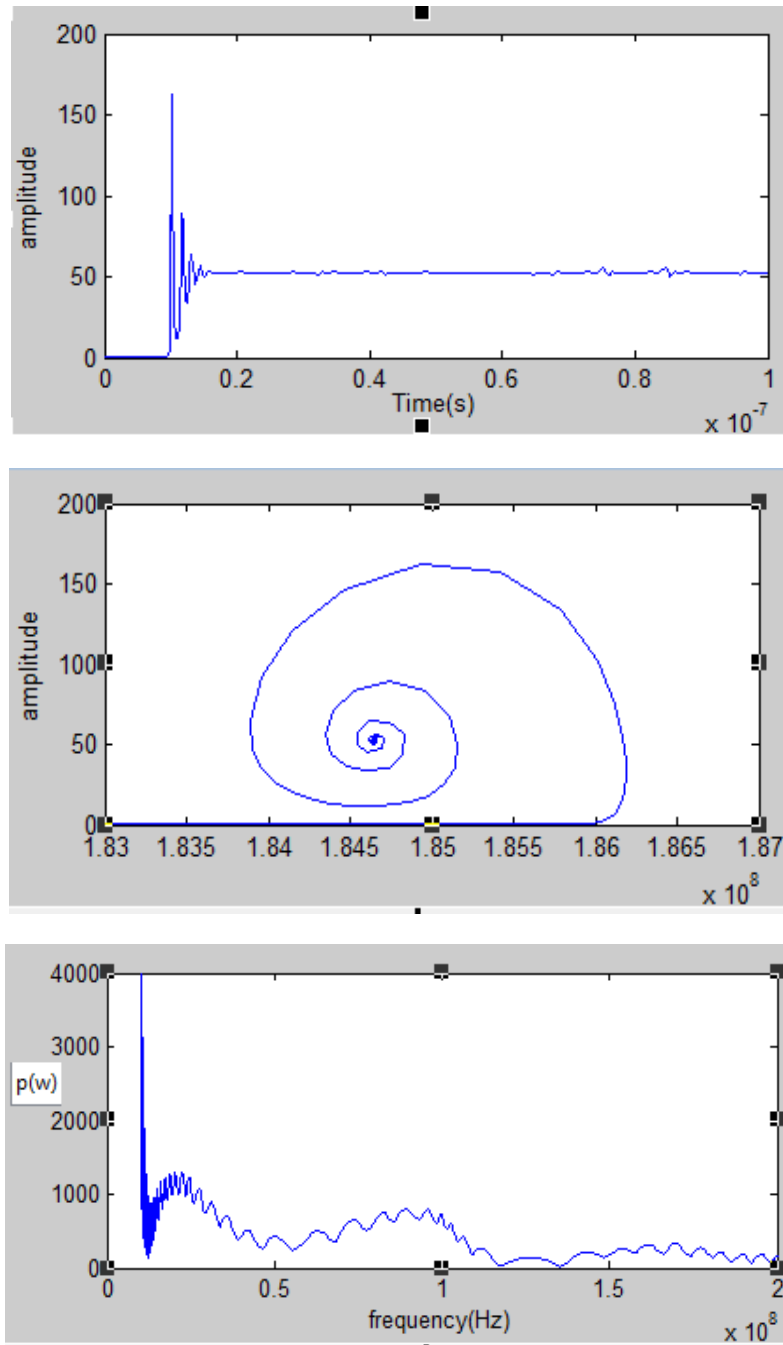
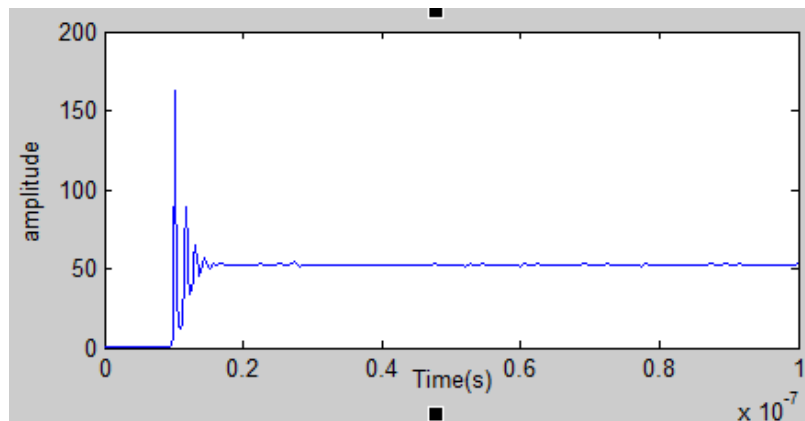


Fig. 3 time series of the laser output power, its phase portrait and corresponding FFT spectrum. at  $k=36e^{-6}ns^{-1}$ ,  $i_{dc}=10mA$ ,  $i_{ac}=5mA$ ,  $f_m=100e^6$  Hz.



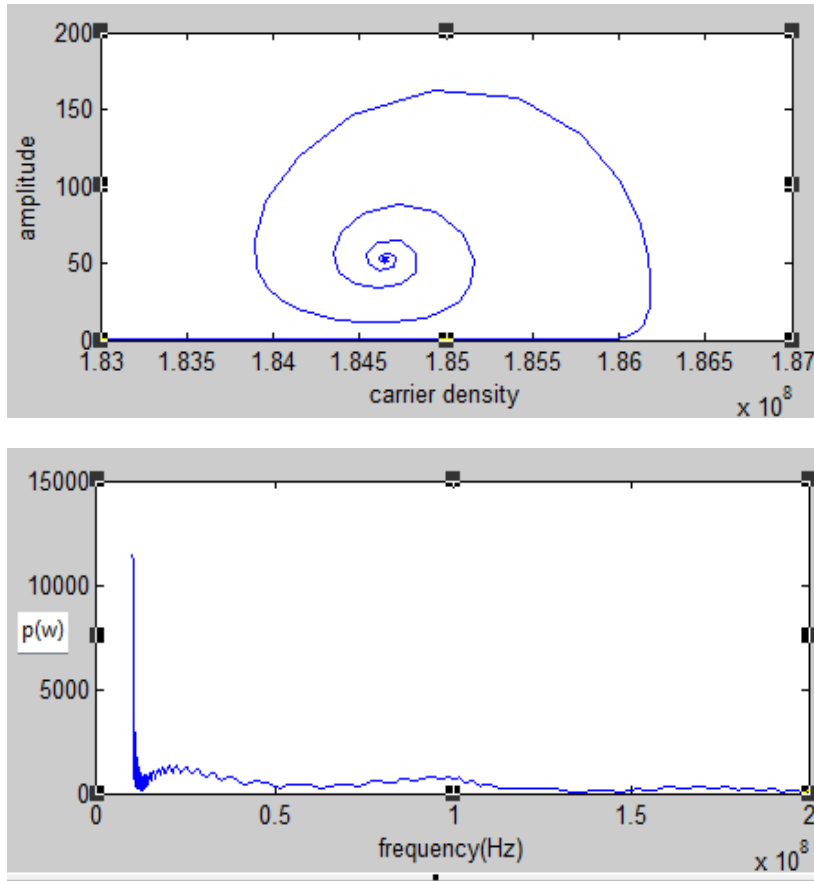
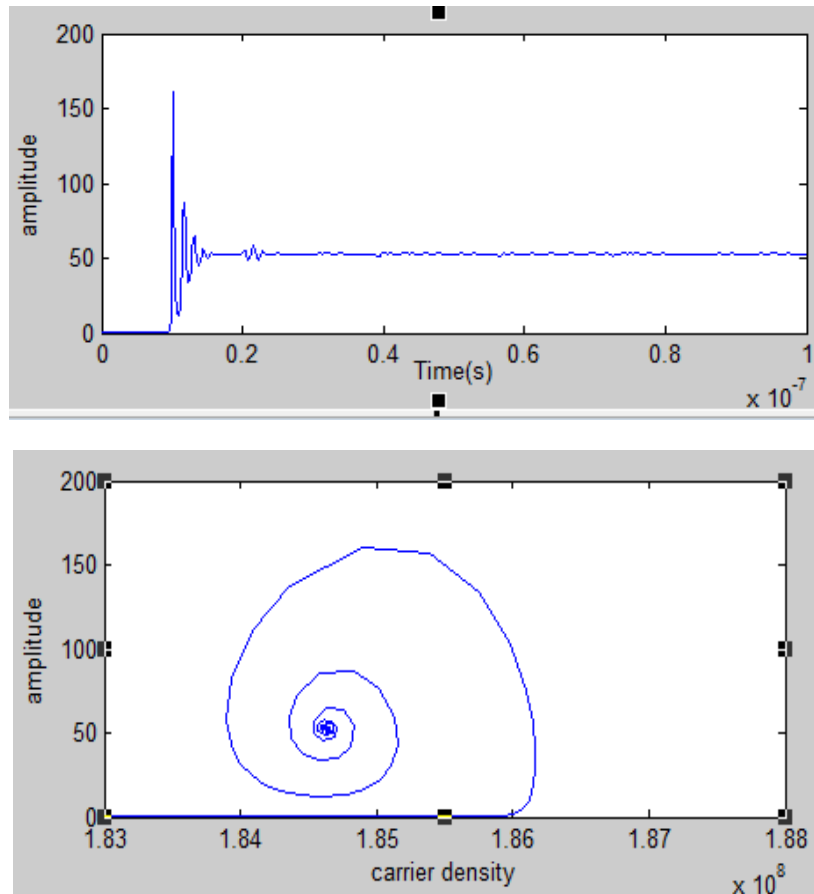


Fig. 4 time series of the laser output power, its phase portrait and corresponding FFT spectrum. at  $k= 36e^{-4} \text{ ns}^{-1}$ ,  $i_{ac} = 10\text{mA}$ ,  $i_{ac} = 5\text{mA}$ ,  $f_m = 100e^6 \text{ Hz}$ .



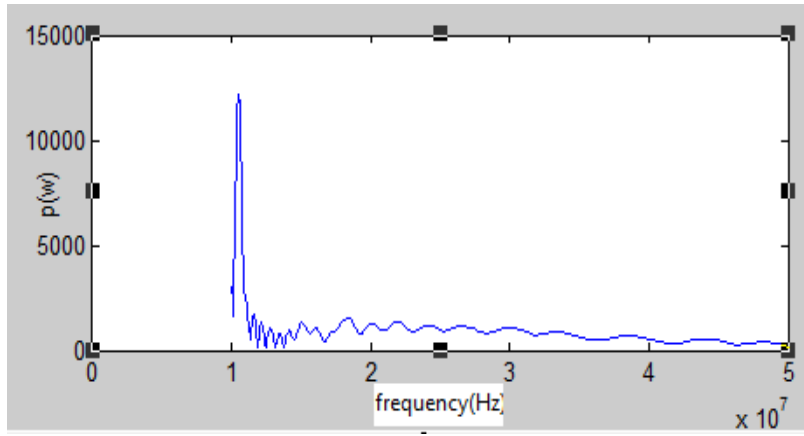


Fig. 5 time series of the laser output power, its phase portrait and corresponding FFT spectrum. at  $k= 36e^{-2} \text{ ns}^{-1}$ ,  $i_{dc} = 10\text{mA}$ ,  $i_{ac} = 5\text{mA}$ ,  $f_m = 100e^6 \text{ Hz}$ .

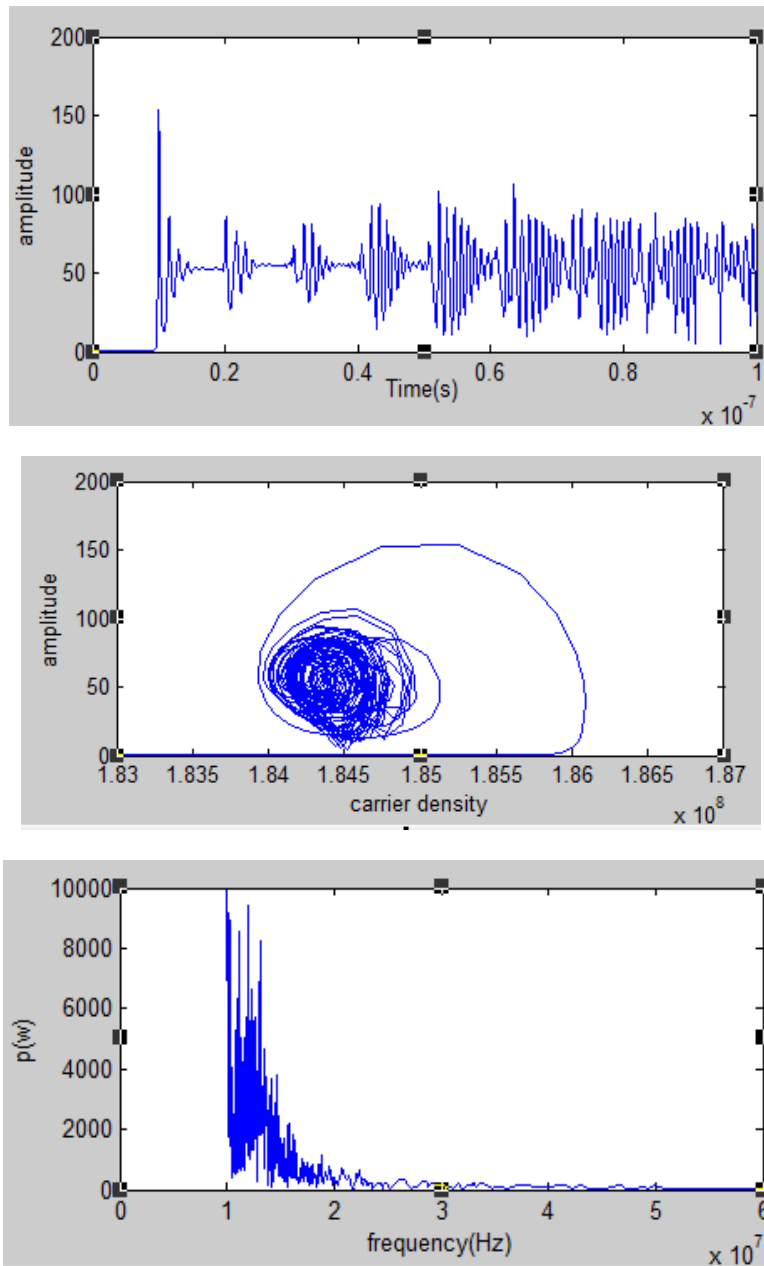


Fig. 6 time series of the laser output power, its phase portrait and corresponding FFT spectrum. at  $k= 36e^{-1} \text{ ns}^{-1}$ ,  $i_{dc} = 10\text{mA}$ ,  $i_{ac} = 5\text{mA}$ ,  $f_m = 100e^6 \text{ Hz}$ .

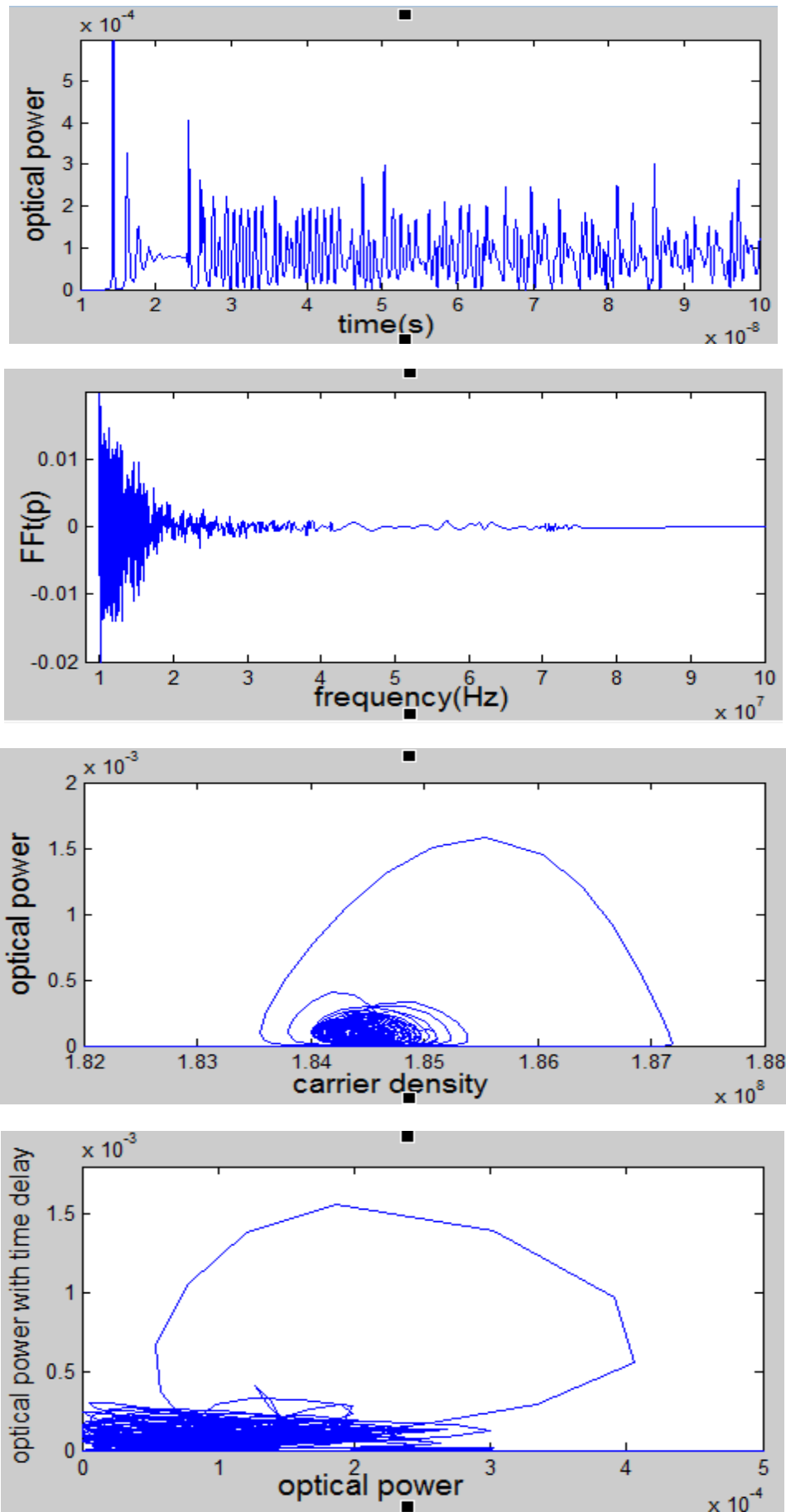


Fig. 7 The time series of the laser output power, its corresponding FFT spectrum and phase portrait. At  $k= 36e^{-1}ns^{-1}$ ,  $i_{dc}=10mA$ ,  $i_{ac} = 5mA$ ,  $f_m = 100e^6$  Hz.

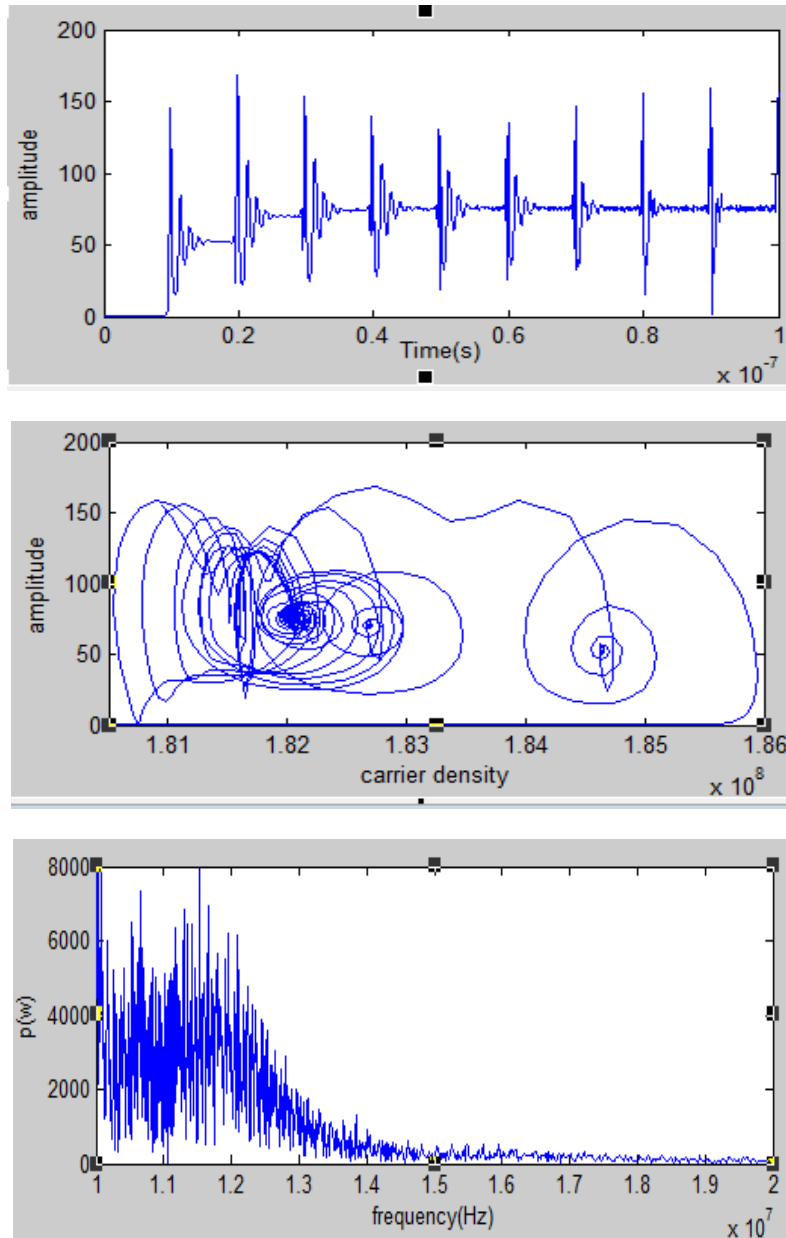
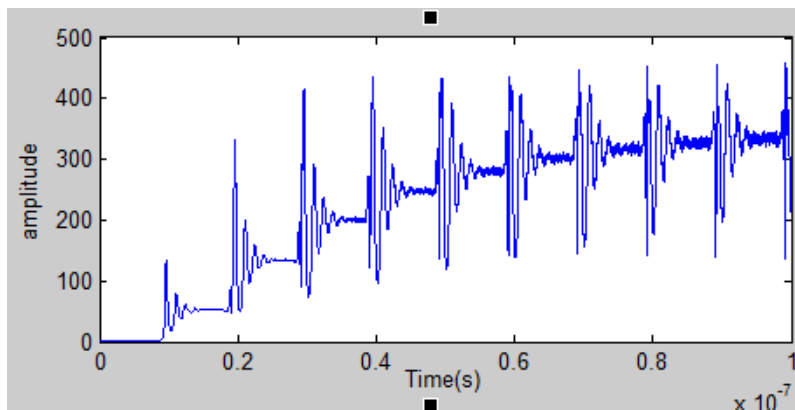


Fig. 8 time series of the laser output power, its phase portrait and corresponding FFT spectrum. at  $k= 36 \text{ ns}^{-1}$ ,  $i_{ac}=10\text{mA}$ ,  $i_{dc}= 5\text{mA}$ ,  $f_m = 100\text{e}^6 \text{ Hz}$ .



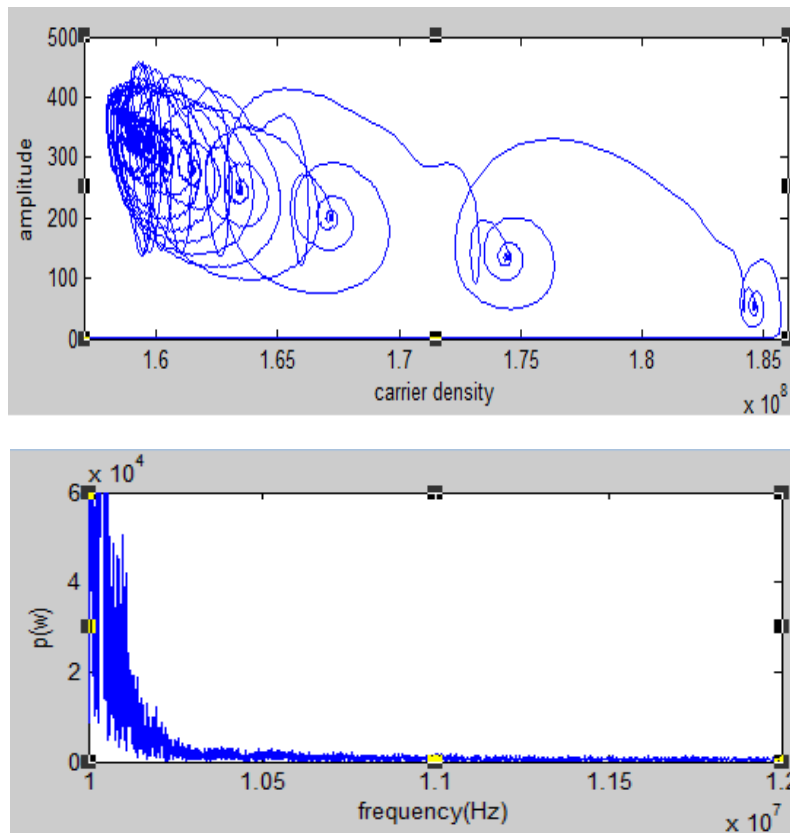


Fig. 9 time series of the laser output power, its phase portrait and corresponding FFT spectrum. at  $k= 360 \text{ ns}^{-1}$ ,  $i_{dc} =10\text{mA}$  ,  $i_{ac} = 5\text{mA}$ ,  $f_m = 100\text{e}^6 \text{ Hz}$ .

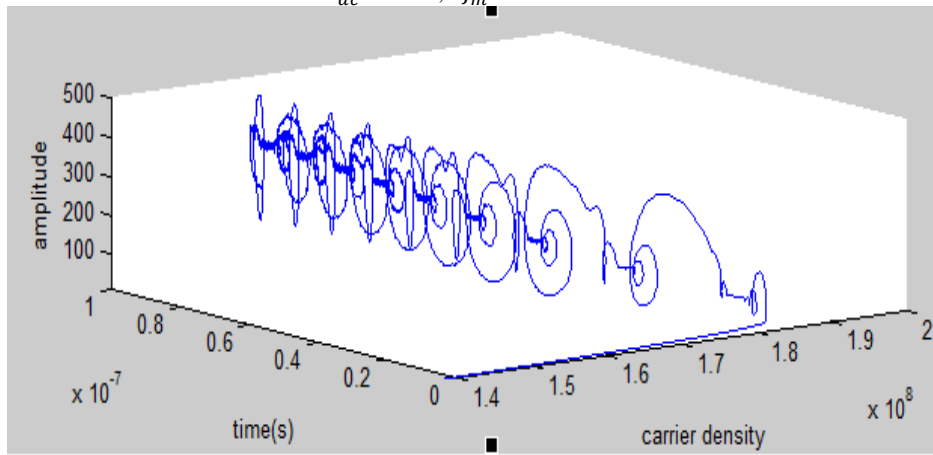


Fig. 10 phase portrait. at  $k= 360 \text{ ns}^{-1}$ ,  $i_{dc} =10\text{mA}$  ,  $i_{ac} = 5\text{mA}$ ,  $f_m = 100\text{e}^6 \text{ Hz}$ .

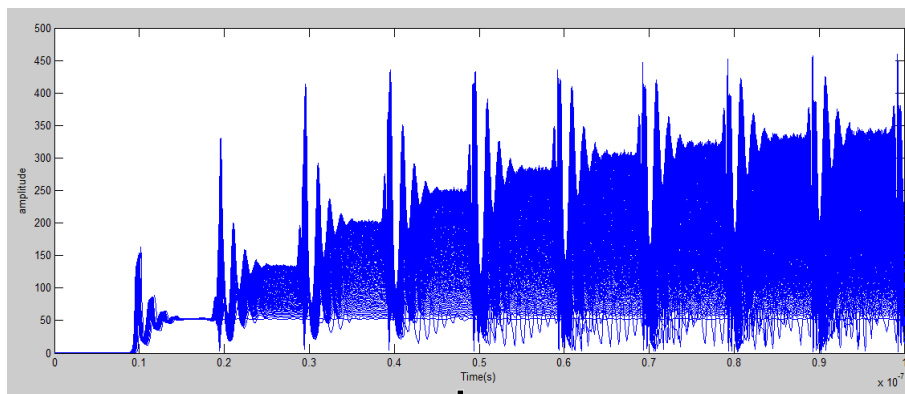


Fig. 11 time series of the laser amplitude.at  $k= 360 \text{ ns}^{-1}$ ,  $i_{dc} =10\text{mA}$  ,  $i_{ac} = 5\text{mA}$ ,  $f_m = 100\text{e}^6 \text{ Hz}$ .

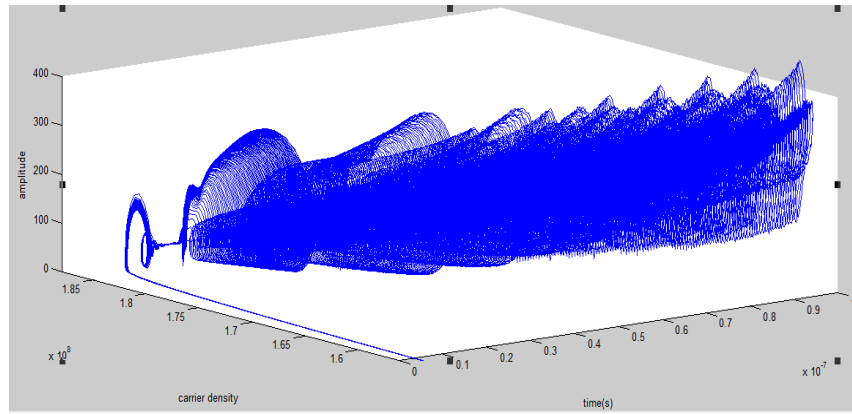


Fig. 12 phase portrait for amplitude versus carrier density and time. at  $k= 360 \text{ ns}^{-1}$ ,  $i_{dc}=10\text{mA}$  ,  $i_{ac} = 5\text{mA}$ ,  $f_m = 100\text{e}^6$  Hz.

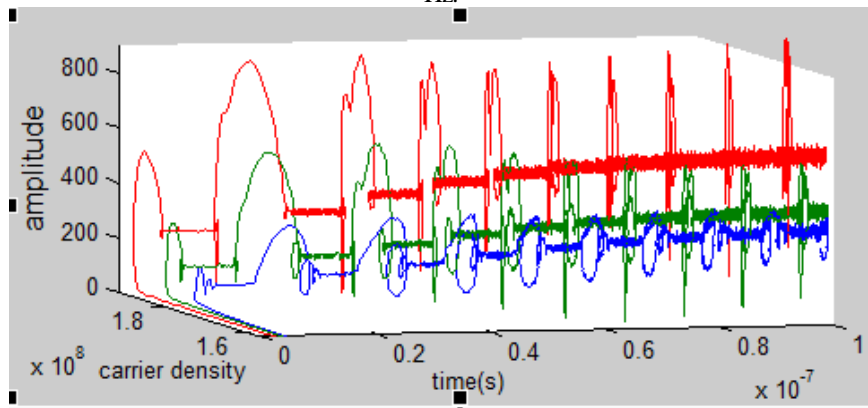


Fig. 13 phase portrait for amplitude versus carrier density and time. at  $k= 360 \text{ ns}^{-1}$ ,  $i_{dc}=10\text{mA}$  ,  $i_{ac} = 5\text{mA}$ ,  $f_m = 100\text{e}^6$  Hz.